ACS APPLIED MATERIALS & INTERFACES

www.acsami.org

Research Article

Preparation of High Thermal Conductivity Graphene Films by Rapid Reduction with Low Energy Consumption

Ning Li, Junhao Liu, Wenfang Zeng, Yawei Xu, and Jing Li*

Cite This: https://doi.org/10.1021/acsami.4c10163

Read Online

ACCESS | Metrics & More | Article Recommendations | Supporting Information

ABSTRACT: In the domain of smart electronic devices, graphene films play a pivotal role due to their flexibility and high thermal conductivity. Within the realm of fabricating highly thermally conductive graphene films, Joule heating technology has garnered significant attention because of its capability for rapid temperature elevation and reduction of graphitization duration. However, substantial gas emission occurs during the reduction of graphene oxide films using this method, leading to immediate combustion and film fracturing, thereby limiting the rapid and uninterrupted production of graphene films. To address this challenge, a rapid reduction preparation process is introduced. This process initiates with a two-step reduction of graphene oxide films employing a reducing agent to establish gas escape pathways within the graphene films beforehand. Subsequently, the film is pressurized and Joule-heated using a graphite plate, with the entire heating process lasting only 800 s. The resulting graphene film exhibits a remarkable thermal conductivity of up to 1012W/(m·K). This method enhances the production efficiency of high thermal conductivity graphene films and is expected to further reduce production costs.

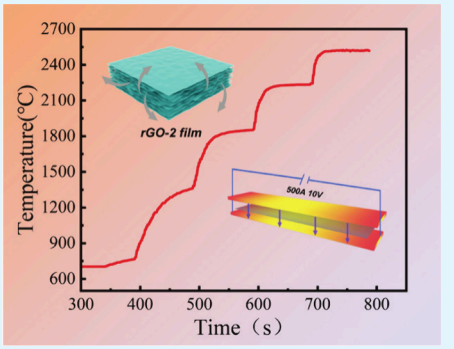

KEYWORDS: *reduced graphene oxide films, Joule heat, gas escape channels, restore quickly, high thermal conductivity*

1. INTRODUCTION

In recent years, the consumer market has witnessed a gradual integration of smart folding-screen mobile phones and wearable devices, facilitated by the widespread adoption of 5G technology and notable enhancements in chip performance.[1−4] Despite their compact internal design, these state-of-the-art devices often face challenges associated with excessive heat generation from chips and subsequent performance degradation during prolonged usage.[5,6] To mitigate this issue, graphene thermally conductive films, originally prominent in the aerospace sector, have been incorporated into the manufacturing process of high-grade electronics.[7,8] In commercial production, graphite films exhibiting exceptional thermal conductivity are typically fabricated using polyimide (PI) films, which undergo sintering in a carbide furnace at temperatures reaching up to 3000 °C for several hours.[9] Alternatively, another method employs a redox process wherein graphite powder undergoes oxidation to strip off graphene oxide (GO). Subsequently, following the formation of a thin film, the GO is reduced at similarly high temperatures to yield graphene films (GF) characterized by superior thermal conductivity.[10] This technological advancement has notably enhanced the properties of thermally conductive films. However, both aforementioned preparation methods necessitate prolonged exposure to elevated temperatures, resulting in substantial energy consumption. Therefore, exploring novel approaches to mitigate energy consumption during the high-temperature reduction stage and further reducing production costs are imperative to facilitate the widespread adoption of high thermal conductivity graphene films in the electronics market.

In efforts to diminish energy consumption during graphene film preparation, researchers have explored an array of innovative rapid-temperature-elevation techniques. These methods include microwave reduction, laser irradiation, and Joule heating methods.[11−15] Among these, the CO2 laser technique has been investigated, wherein rapid irradiation on polyimide (PI) films instantly elevates the laser temperature to permeate the PI films, albeit resulting in inadequate graphitization.[16] Notably, the laser reduction process exhibits linear characteristics, necessitating enhancements in the overall graphitization efficiency of the PI film. Conversely, Zhao et al. pursued an alternative approach by superimposing Reduced Graphene Oxide (rGO) films onto GO films. They successfully imparted reduced graphene traces onto the GO surface using microwave ovens, achieving rapid heating within 4 to 5 s.[16] The resultant graphite traces on the PI film surface were then

Received: June 20, 2024
Revised: October 2, 2024
Accepted: October 10, 2024

heated via microwave ovens, facilitating the graphitization process. However, as the GO film itself does not absorb microwaves, relying on the rGO film for heat transfer, the reduction effect within the GO film is constrained. Hence, the optimization of microwave fast reduction techniques to achieve uniform temperature distribution warrants further investigation. Peng et al. employed a calendering process to flatten resultant fullerene structures, screening large-sized GO and subjecting them to a pressure of 300 MPa post high-temperature graphitization treatment at 3000 °C.[17] This process endowed the Graphene Films (GFs) with a certain degree of flexibility, yielding GFs exhibiting a thermal conductivity of 1940 ± 113 W/(m·K), showcasing excellent thermal conductive properties. On another front, Gao et al. devised a continuous Joule heating device employing two graphite rollers to enable the continuous production of high-thermal-conductivity GFs.[18] By rotating the rollers and applying direct current to the rGO, the resulting Joule heating temperature reached 2443 °C. The maximum thermal conductivity of the obtained GF reached 1285 ± 20 W/(m·K), with this continuous production method offering the potential for large-scale production. These studies not only advance GF preparation technology but also establish a foundation for the application of high thermal conductivity GF in electronic devices.

There are still some problems that need to be solved in the rapid reduction stage of GO by laser, microwave, or Joule-thermal methods, such as the income plete reduction of the interior of the film by laser and microwave methods, as well as the destruction of the lamellar structure of GO by direct reduction.[11,19,20] Therefore, chemical reduction treatments or pretreatments at around 800 °C are required before these rapid reduction methods are employed, and In order to improve the thermal conductivity, a cold pressing treatment of 300 MPa is usually required to densify the structure.[15,21−23] Although fast reduction techniques offer new ways to prepare high-performance graphene films, technical and technological challenges need to be solved in order to realize their potential.

In this study, an innovative Joule heating device is introduced for the rapid reduction of graphene films. The approach begins with two chemical reductions of GO to produce rGO, aimed at augmenting sheet layer spacing within the film and establishing gas escape channels to prevent damage from rapid gas flushing during reduction. Subsequently, the rGO film is sandwiched between two layers of graphite sheets and undergoes uniformly elevated temperature thermal annealing treatment facilitated by heat conduction and radiation. Compared to the conventional method of directly heating rGO with direct current, this technique effectively mitigates temperature discrepancies and potential fracture issues stemming from uneven resistance distribution within the film. The entire thermal annealing process lasts 800 s, enabling rapid and energy-efficient graphene film preparation. The resulting graphene film boasts a thermal conductivity of 1012 W/(m·K), paving the way for applications necessitating high thermal conductivity and low power consumption. This method unveils promising prospects for the integration of high thermal conductivity graphene films within the consumer electronics industry.

2. EXPERIMENTAL SECTION

2.1. Materials. Scalar graphite (100 mesh) used in the experiments was purchased from Aladdin Reagent Company, hydriodic acid (HI, 57 wt %) was from Inokai Science and Technology Company, Beijing, China, concentrated sulfuric acid (H2SO4, 98 wt %), concentrated hydrochloric acid (HCl, 37 wt %), potassium permanganate (KMnO4, 99 wt %), hydrogen peroxide (H2O2,30 wt %), hydrochloric acid (HCl, 5%), ethanol (C2H5OH), were purchased from Guangzhou Chemical Reagent Factory, China. 99%), were purchased from Guangzhou Chemical Reagent Factory, China.

2.2. Preparation of rGO and GF Films. Preparation of reduced graphene oxide (rGO): The preparation of GO is mainly based on Dong' improvement of Hummers' method to obtain large-size GO,[24] the specific preparation process is to add 2g of 100 mesh graphite powder to 85 mL H_2SO_4 and 8.5 g $KMnO_4$ mixture, and let it stand for 24 h. After that, put it into 500 mL of iced water, and then add H_2O_2 to produce golden-yellow semiexfoliated large-size GO, add 20 mL of dilute hydrochloric acid to remove excess metal ions,, and after 4−5 times of deionized water washing, get completely exfoliated large-size GO, let it settle and remove the upper layer of clear liquid to get brown large-size GO. And the SEM image of the large-size GO was taken (Figure S2, Supporting Information). The rGO film sheet layer spacing was increased using the team's previously investigated method of secondary reduction of GO films.[25] This was done by reducing the GO films in 57% hydriodic acid (HI) solution for 1 h. The GO films were continued by placing them in a hydrothermal reactor, immersing them in 57% HI solution, and reducing them for 3 h at 160 °C to obtain the rGO films. The rGO film was washed in ethanol solution for 3−4 times to remove the residual HI in the film, and the rGO film was dried at 55 °C to obtain the final rGO film.

Preparation of reduced graphene film (GF): Figure S1 illustrates the schematic diagram of the rapid high-temperature reduction device. The reduction process was conducted within a sealed metal cavity using argon gas, employing a graphite heating sheet measuring 100 × 20 × 2 mm. To facilitate real-time temperature monitoring of the heating table, a sapphire window sheet was installed at the bottom of the stainless steel cavity, enabling temperature measurements via an infrared thermometer. Square graphite electrodes clamped the ends of the heating table. rGO film was cut into 80 × 20 mm strips and positioned between two graphite sheets, secured to the electrodes using graphite bolts. The graphite heating pads were connected to a 40 V500A autoregulated power supply. The heating process of the graphite heating sheet was precisely controlled through staged heating by adjusting the power supply's output current, achieving temperatures up to 2500 °C. Additionally, to assess the impact of rapid high-temperature reduction on internal graphitization, temperature-controlled reductions were performed on rGO at peak currents of 400A and 500A, respectively. Postreduction, rGOs were obtained and named GF-2200 and GF-2500 after roller pressing.

2.3. Characterization. The micromorphology of the samples was examined using a cold field emission scanning electron microscope (SEM) (Hitachi SU8200) at an accelerating voltage of 10.0 kV. Raman spectroscopic measurements were conducted by H.J.Y. LabRAM Aramis at a laser wavelength of 532 nm. X-ray photoelectron spectroscopy (XPS) measurements were carried out on an Axis Ultra DLD to quantify the elemental content of the samples, with Al Kα utilized as the X-ray source. X-ray diffraction (XRD) tests were performed to analyze the sample structure using a Cu-targeted Kα source at a wavelength of 0.15406 nm, a test voltage of 40 kV, and a tube current of 40 mA. The thermal diffusion coefficient of the samples was determined using a flash-method thermal conductivity meter (Netzsch LFA 467), while infrared thermal imaging (FLIR C5) was employed for sample thermal conductivity distribution testing.

3. RESULTS AND DISCUSSION

As depicted in Figure 1, the graphene oxide (GO) obtained via the modified Hummers method underwent reduction in a 57% HI solution. After 3 h of reduction at room temperature, the majority of oxygen-containing groups within the GO film were removed, yielding the preliminary reduced graphene oxide film, denoted as rGO-1. Subsequently, rGO-1 was immersed in a

https://doi.org/10.1021/acsami.4c10163
ACS Appl. Mater. Interfaces XXXX, XXX, XXX−XXX

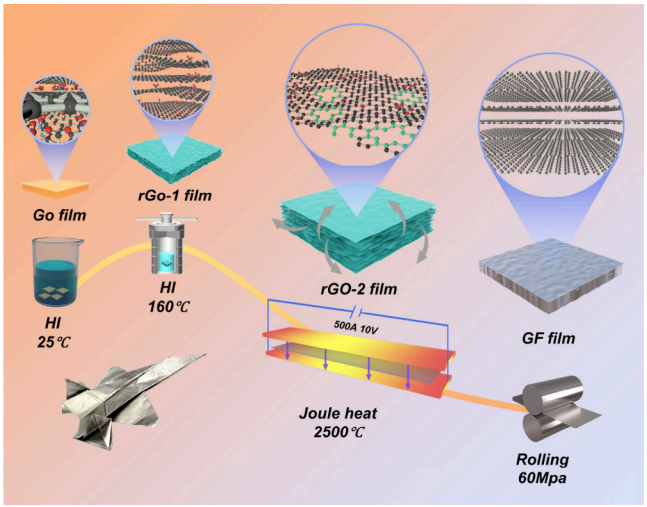

Figure 1. Schematic diagram of the preparation process.

57% HI solution and subjected to continued reduction at 160 °C in a hydrothermal reactor for 3 h. This process aimed to further increase the internal interlayer distances in rGO-1 and establish gas escape channels in anticipation of rapid reduction. Consequently, the thickness of the resulting rGO-2 significantly surpassed that of rGO-1. The second chemical reduction introduced numerous vacancies and defects within the graphene lamellae, commonly addressed by scholars through the augmentation of the carbon source and its decomposition at high temperatures.[26−28] This repair method often necessitates ultrahigh temperatures (~3000 °C) to eliminate excess elements of the carbon source, significantly complicating the reduction process. Joule heating facilitates the cleavage of graphene carbon atoms at the defective edges of graphene sheets under high temperatures, with the liberated carbon atoms effectively repairing internal sheet defects. This mechanism enables defect rectification within graphene sheets without the need for additional carbon sources, culminating in the formation of a continuous and intact graphene lattice structure.[29,30]

To prevent the disruption of graphene layer stacking caused by the rapid outflow of gas within the film during temperature elevation, a temperature rise procedure for the graphite heater access current was devised. The variation of rGO-2 film reduction temperature over time is illustrated in Figure. S3(a), while the fluctuation of the access current over time is depicted in Figure S3(b). The infrared thermometer, with a measurement range of 700 to 3000 °C, was utilized to record the temperature variation over time, beginning at the point when the heating plate reached 700 °C. The entire heating process comprises 8 segments, with each segment lasting 100 s, resulting in a total reduction time of 800 s. Initially, the current difference between the first 4 heating segments is set at 20A. Upon reaching the fourth temperature segment at 870 °C, the subsequent 4 program segments entail rapid heating, with each heating segment featuring a current difference of 100A. Ultimately, when the maximum access current of 500A is attained, the power supply voltage is set at 30 V, achieving a peak reduction temperature of 2500 °C. At this juncture, the heating power reaches 15KW, and the total energy consumption of the reduction process amounts to 1.55KWh. By contrast, traditional graphitization furnace heating rates typically range from 35 to 300 °C/h, with reduction durations spanning 3−12 h. Thus, this method abbreviates the high-temperature reduction duration by more than 90%. Scaling up the reduction size merely requires enhancements to the graphite heating table and stainless-steel chamber, facilitating the mass production of graphene films with minimal energy consumption.

Scanning electron microscopy (SEM) images revealed that graphene oxide (GO) films exhibited tightly packed interlayers with thicknesses ranging from 15 to 22 μm (Figure 2a).

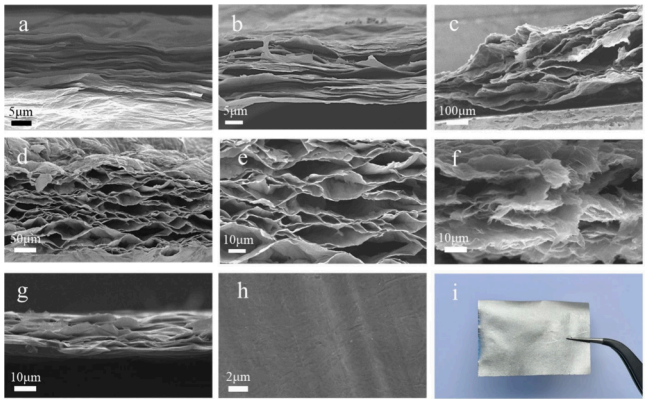

Figure 2. (a) SEM image of GO cross-section. (b) SEM image of rGO-1 cross-section. (c)−(e) SEM images of rGO-2 cross-section. (f) SEM image of cross-section before GF roll pressing. (g) SEM image of cross section after GF roll pressing. (h) SEM image of the surface after GF roll pressing. (i) GF diagram.

Chemical reduction with HI at ambient temperature resulted in an increased interlayer spacing of the rGO-1 films, expanding their thickness to 20−25 μm (Figure 2b). Hydrothermal treatment with HI at 160 °C further enlarged the interlayer gap in rGO-2 films, increasing their thickness to 300−350 μm (Figure 2c). Continuous delamination and channels were observed at various locations in rGO-2 (Figure 2d), with magnified images indicating that the internal channels possessed significant depth (Figure 2e). This treatment not only facilitates the removal of oxygen-containing functional groups from rGO-1 but also creates channels for gas escape, which is critical for rapid reduction during Joule heating. Following rapid reduction under controlled temperature conditions, the thickness of rGO-2 remained relatively stable, and the cross-sectional structure preserved its lamellar configuration without further expansion of the interlayer voids (Figure 2f). After roll pressing, the graphene film (GF) exhibited a compact and ordered internal structure (Figure 2g), with a thickness reduced to 18−22 μm, closely approximating the thickness of the initial GO film. These findings suggest that the two-step HI reduction process effectively mitigates structural damage caused by gas release, facilitates rapid gas expulsion, reduces thermal resistance, and increases GF density. The flat and wrinkle-free surface of the calendered films (Figure 2h and 2i) further indicates that this method avoids producing a loose and porous film interior. The cross-section of the calendered GF exhibited a dense internal interlayer with orderly sheet stacking, providing efficient thermal and electrical conduction pathways for phonons and photons. Moreover, the dense architecture of the GF endows it with exceptional flexibility, allowing it to endure 300 cycles of 180° end-to-end bending without exhibiting signs of fracture.

https://doi.org/10.1021/acsami.4c10163
ACS Appl. Mater. Interfaces XXXX, XXX, XXX−XXX

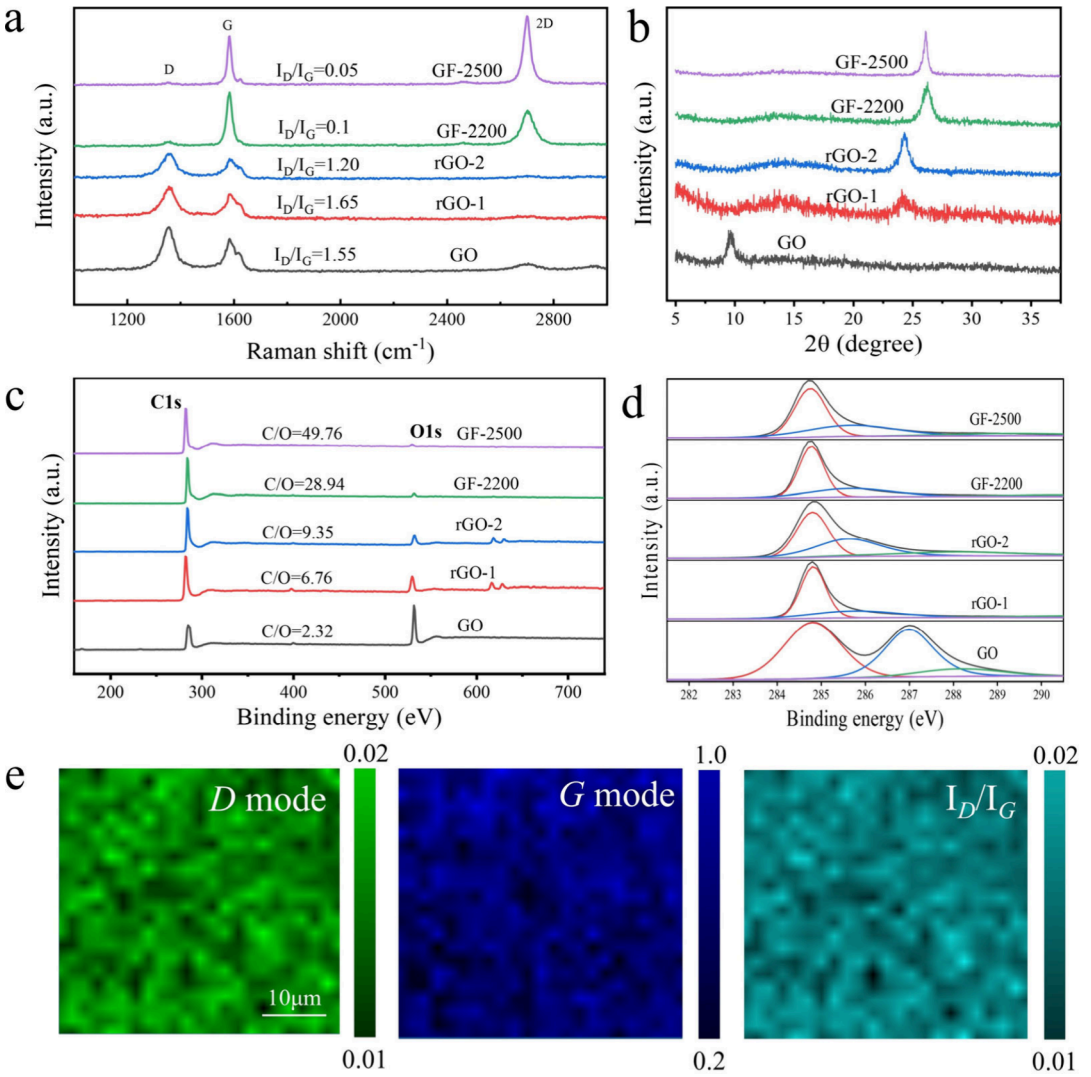

Figure 3. (a) Raman spectra of GO, rGO-1, rGO-2, GF-2200, and GF-2500. (b) XRD spectra of GO, rGO-1, rGO-2, GF-2200, and GF-2500. (c) XPS measurement spectra of GO, rGO-1, rGO-2, GF-2200, and GF-2500. (d) GO, C 1s deconvolution spectra of rGO-1, rGO-2, GF-2200, GF-2500. (e) Raman mapping of D band, G band, and I_D/I_G of the GF-2500.

To thoroughly investigate the impact of the rapid high-temperature reduction technique on the internal structure of GF, X-ray photoelectron spectroscopy (XPS) and Raman spectroscopy tests were conducted on rGO and its resultant graphene film (GF). Raman spectroscopy results (Figure 3a) reveal that the intensity of GF-2500 obtained through high-temperature rapid reduction significantly decreases at the defect peak (D peak, 1350 cm^{-1}) compared to rGO-1, while exhibiting a higher intensity at the G peak (1580 cm^{-1}) of the graphene lattice. Comparing the D-peak to G-peak intensity ratio (I_D/I_G) of rGO-1 and rGO-2, a decrease from 1.65 to 1.20 suggests a substantial effect in repairing the defects of rGO-1 at 160 °C. The D-peak to G-peak intensity ratios of 0.1 and 0.05 for GF-2200 and GF-2500 respectively indicate that rapid high-temperature reduction effectively rectified graphene defects. Notably, the intensity of the 2D peak (2680 cm^{-1}) of GF-2500 exceeds that of the G peak, signifying that the fast high-temperature reduction still produces a stable graphene lamellar stacking structure.[31,32] To assess the internal homogeneity of GF-2500, Raman mapping was utilized to observe the D-peak, G-peak, and I_D/I_G normalization, revealing a uniform internal structure at the micron level (Figure 3e).

The reduction effect was further verified through X-ray diffraction (XRD) analysis (Figure 3b). The diffraction peak of GO was positioned at 9.5°, while the diffraction peak of rGO-2 after two HI reductions shifted to a higher angle at 24.1° (layer spacing of 0.369 nm), indicating the removal of more oxygen-containing functional groups during the chemical reduction process. Eventually, both GF-2200 and GF-2500 exhibited diffraction peaks near 26.5° (layer spacing 0.336 nm), aligning with the standard diffraction peak position of graphite, affirming the realization of GF graphitization through rapid high-temperature reduction. In XPS analysis (Figure 3c), the carbon−oxygen ratios (C/O) of rGO-1 and rGO-2 were 6.76 and 9.35 respectively, with the O content of rGO-2 decreasing by 5% compared to rGO-1. Meanwhile, the C/O ratios of GF-2200 and GF-2500 markedly increased to 28.94 and 49.76, respectively, indicating a reduction in oxygen-containing groups before rapid reduction, thereby facilitating subsequent high-temperature reduction. The creation of an oxygen-free environment during the high-temperature reduction stage, resulting from the reduction of oxygen content inside the film after the two-step chemical reduction and the rapid escape of interlayer gases, reduced the difficulty of reduction. This

https://doi.org/10.1021/acsami.4c10163
ACS Appl. Mater. Interfaces XXXX, XXX, XXX−XXX

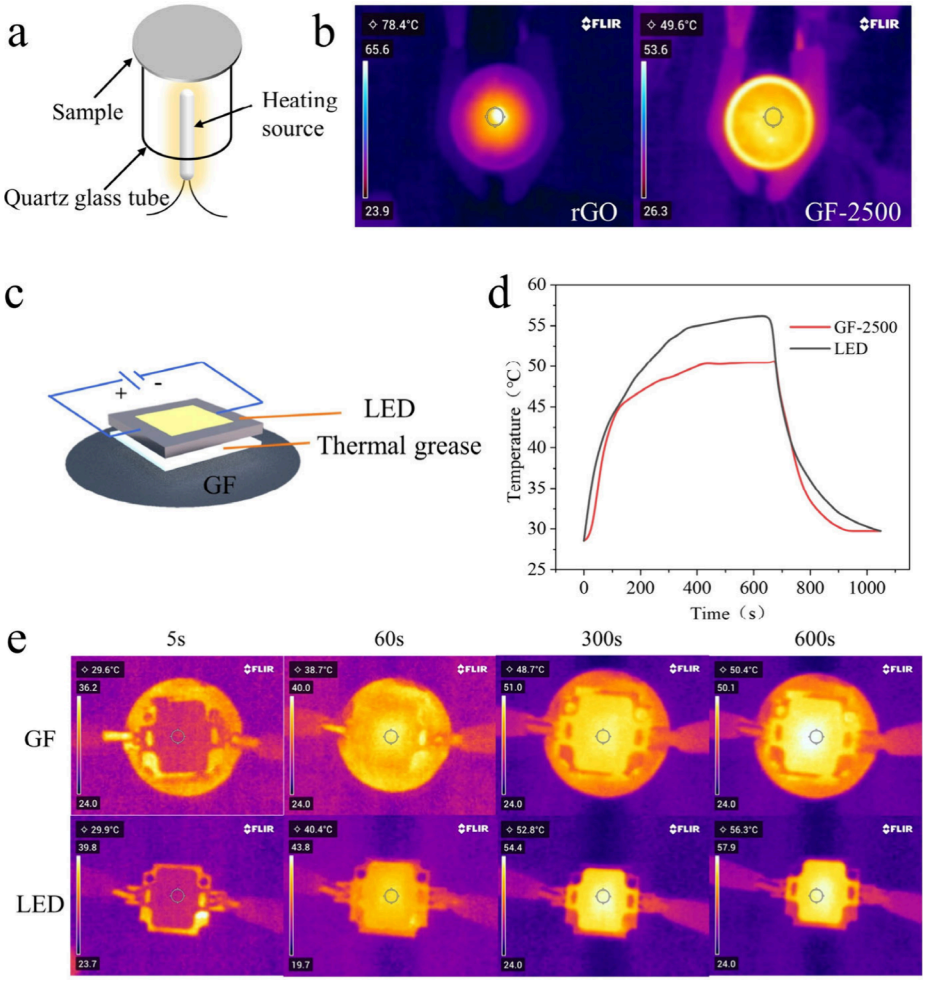

Figure 4. (a) Schematic diagram of the test setup. (b) Infrared thermal image of rGO, Gf-2500 film. (c) Schematic diagram of the test setup. (d) LED heat dissipation graph. (e) Temperature change of the infrared thermal image of the LED surface under GF-2500 heat dissipation and no GF heat dissipation.

conclusion was further supported by the C 1s deconvolution spectra (Figure 3d). In conclusion, the characterization results show that the transient high temperature generated by the fast high-temperature reduction method in a short period of time is able to achieve the complete reduction of rGO, and that the high temperature is still a key factor in determining the degree of graphene graphitization.

The thermal diffusion coefficients of GF-2200 and GF-2500 were measured to be 476 mm^2/s and 580 mm^2/s, respectively, using a laser flash method thermal conductivity meter (Netzsch LFA 467). The densities of the samples were determined to be 1.86 g/cm^3 and 2.01 g/cm^3, respectively. Subsequently, calculations yielded thermal conductivities of 690W/(m·K) and 1012W/(m·K) for the two samples. These results suggest that constructing a gas escape channel before rapid reduction can mitigate the formation of microair pockets induced by Joule heat, thereby enhancing interlayer compactness of the film and yielding high-density graphene films without the need for excessive pressure during calendering. From the aforementioned characterization results, it is inferred that high temperature remains pivotal for achieving complete graphene lattice structure. Furthermore, the two-step chemical reduction pretreatment of GO, by increasing internal interlayer spacing and preemptively releasing excess oxygen-containing groups, contributes to reducing interlayer gaps in the GF film, enhancing its internal compactness, and ultimately improving GF thermal conductivity.

In order to compare the heat dissipation effect of high thermal conductivity GF in practice, the center of the film was heated using a Led heating rod, and the heating power was adjusted so that when the LED heating rod reached 160 °C, the film was placed 5 mm directly above the heating rod, and the schematic diagram of the device is shown in Figure 4a. The heating temperature at the film's center was recorded until the temperature change stabilized, and the average temperature performance of rGO and GF-2500 was compared using an infrared camera (Figure 4b). Compared with rGO, the center temperature of GF-2500 decreased by 28.8 °C, and the overall surface temperature distribution of GF-2500 was more uniform. Furthermore, to validate the heat dissipation ability of GF-2500, the back of the LED light was coated with thermally conductive silicone grease, and a 20 mm diameter GF-2500 was applied. The surface temperature of the LED lamp was recorded under the same power conditions, and the schematic diagram of the device is shown in Figure 4c. Figure 4d shows the LED heat dissipation temperature curve. The test results revealed that, 10 min after, the surface temperature of the LED bulb with no GF thermal film decreased by 6 °C. Conversely, with the GF-2500, the heat dissipation was faster, evidenced by the time it took for LEDs with GF-2500 to return

https://doi.org/10.1021/acsami.4c10163
ACS Appl. Mater. Interfaces XXXX, XXX, XXX−XXX

from a constant temperature of 50.6 °C to room temperature, shortened by 42.8%. This conclusion is supported by the infrared image in Figure 4e. These results demonstrate that GF can effectively reduce the operating temperature of high heat-generating electronic components, and by increasing the area of GF, further enhancement of heat dissipation efficiency can be achieved.

4. CONCLUSIONS

In this study, we adopted a two-step reduction method to treat GO, which significantly increased the interlayer distance of the sheet and provided the necessary gas escape channel for the subsequent Joule-heated rapid high-temperature reduction. This design avoids the damage to the internal structure of the film caused by the large amount of gas that suddenly rushes out during the rapid reduction stage. During the reduction process, we utilize the double-layer graphite plate to directly heat the film, and by controlling the power output, we realize the strategy of slowly increasing the temperature in the first half of the heating process, and rapidly increasing the temperature to 2500 °C in the second half. The graphene film was tested to have a thickness of 20 μm, a density of 2.01 g/cm^3, and outstanding thermal conductivity with an in-plane thermal conductivity of 1012 W/(m·K). The Joule-heat fast reduction method proposed in this study not only improves the efficiency of GO reduction, but also effectively avoids energy waste in the reduction process. This method reduces the production cost of high thermal conductivity reduced graphene oxide films while providing new possibilities for the expansion of high thermal conductivity graphene films in the consumer electronics application market.

■ ASSOCIATED CONTENT

Supporting Information

The Supporting Information is available free of charge at https://pubs.acs.org/doi/10.1021/acsami.4c10163.

Schematic diagram of high-temperature rapid reduction device (Figure S1); SEM image of graphene oxide (Figure S2); and (a) plot of reduction temperature versus time and (b) plot of voltage versus time (Figure S3) (PDF)

■ AUTHOR INFORMATION

Corresponding Author

Jing Li − *School of Chemistry and Chemical Engineering, South China University of Technology, Guangzhou 510641, P. R. China; South China University of Technology-Zhuhai Institute of Modern Industrial Innovation, Zhuhai 519000, P. R. China*; Email: ljing@scut.edu.cn

Authors

Ning Li − *School of Chemistry and Chemical Engineering, South China University of Technology, Guangzhou 510641, P. R. China*; orcid.org/0009-0002-0642-2469

Junhao Liu − *School of Chemistry and Chemical Engineering, South China University of Technology, Guangzhou 510641, P. R. China*

Wenfang Zeng − *School of Chemistry and Chemical Engineering, South China University of Technology, Guangzhou 510641, P. R. China*

Yawei Xu − *National Key Laboratory of Spacecraft Thermal Control, Beijing Institute of Spacecraft System Engineering, Beijing 100086, P. R. China*

Complete contact information is available at: https://pubs.acs.org/10.1021/acsami.4c10163

Notes

The authors declare no competing financial interest.

■ ACKNOWLEDGMENTS

This work was supported by the Shanghai Aerospace Science and Technology Innovation Foundation (SAST2022-047).

■ REFERENCES

(1) Khan, R.; Kumar, P.; Jayakody, D. N. K.; Liyanage, M. A Survey on Security and Privacy of 5G Technologies: Potential Solutions, Recent Advancements, and Future Directions. *IEEE Communications Surveys & Tutorials* **2020**, *22*, 196−248.

(2) Chen, W.-Y.; Shi, X.-L.; Zou, J.; Chen, Z.-G. Thermoelectric Coolers for On-Chip Thermal Management: Materials, Design, and Optimization. *Materials Science and Engineering: R: Reports* **2022**, *151*, 100700.

(3) Devi, D. H.; Duraisamy, K.; Armghan, A.; Alsharari, M.; Aliqab, K.; Sorathiya, V.; Das, S.; Rashid, N. 5G Technology in Healthcare and Wearable Devices: A Review. *Sensors* **2023**, *23* (5), 2519.

(4) Xiang, J.; Deng, L.; Zhou, C.; Zhao, H.; Huang, J.; Tao, S. Heat Transfer Performance and Structural Optimization of a Novel Micro-Channel Heat Sink. *Chinese Journal of Mechanical Engineering* **2022**, *35* (1), 38.

(5) Drummond, K. P.; Back, D.; Sinanis, M. D.; Janes, D. B.; Peroulis, D.; Weibel, J. A.; Garimella, S. V. A Hierarchical Manifold Microchannel Heat Sink Array for High-Heat-Flux Two-Phase Cooling of Electronics. *Int. J. Heat Mass Transfer* **2018**, *117*, 319−330.

(6) Habibi Khalaj, A.; Halgamuge, S. K. A Review on Efficient Thermal Management of Air- and Liquid-Cooled Data Centers: From Chip to the Cooling System. *Applied Energy* **2017**, *205*, 1165−1188.

(7) Yang, G.; Yi, H.; Yao, Y.; Li, C.; Li, Z. Thermally Conductive Graphene Films for Heat Dissipation. *ACS Applied Nano Materials* **2020**, *3* (3), 2149−2155.

(8) Xin, G.; Sun, H.; Hu, T.; Fard, H. R.; Sun, X.; Koratkar, N.; Borca-Tasciuc, T.; Lian, J. Large-Area Freestanding Graphene Paper for Superior Thermal Management. *Adv. Mater.* **2014**, *26*, 4521−4526.

(9) Ruan, K.; Guo, Y.; Lu, C.; Shi, X.; Ma, T.; Zhang, Y.; Kong, J.; Gu, J. Significant Reduction of Interfacial Thermal Resistance and Phonon Scattering in Graphene/Polyimide Thermally Conductive Composite Films for Thermal Management. *Research* **2021**, *2021*, 2021.

(10) Renteria, J. D.; Ramirez, S.; Malekpour, H.; Alonso, B.; Centeno, A.; Zurutuza, A.; Cocemasov, A. I.; Nika, D. L.; Balandin, A. A. Strongly Anisotropic Thermal Conductivity of Free-Standing Reduced Graphene Oxide Films Annealed at High Temperature. *Adv. Funct. Mater.* **2015**, *25* (29), 4664−4672.

(11) Jakhar, R.; Yap, J. E.; Joshi, R. Microwave Reduction of Graphene Oxide. *Carbon* **2020**, *170*, 277−293.

(12) Strong, V.; Dubin, S.; El-Kady, M. F.; Lech, A.; Wang, Y.; Weiller, B. H.; Kaner, R. B. Patterning and Electronic Tuning of Laser Scribed Graphene for Flexible All-Carbon Devices. *ACS Nano* **2012**, *6* (2), 1395−1403.

(13) Chen, Y.; Fu, K.; Zhu, S.; Luo, W.; Wang, Y.; Li, Y.; Hitz, E.; Yao, Y.; Dai, J.; Wan, J.; Danner, V. A.; Li, T.; Hu, L. Reduced Graphene Oxide Films with Ultrahigh Conductivity as Li-Ion Battery Current Collectors. *Nano Lett.* **2016**, *16* (6), 3616−3623.

(14) Cheng, Y.; Cui, G.; Liu, C.; Liu, Z.; Yan, L.; Liu, B.; Yuan, H.; Shi, P.; Jiang, J.; Huang, K.; Wang, K.; Cheng, S.; Li, J.; Gao, P.; Zhang, X.; Qi, Y.; Liu, Z. Electric Current Aligning Component Units

during Graphene Fiber Joule Heating. *Adv. Funct. Mater.* **2022**, *32* (11), 2103493.
(15) Huang, P.; Zhu, R.; Zhang, X.; Zhang, W. Effect of Free Radicals and Electric Field on Preparation of Coal Pitch-Derived Graphene Using Flash Joule Heating. *Chemical Engineering Journal* **2022**, *450*, 137999.
(16) Lin, J.; Peng, Z.; Liu, Y.; Ruiz-Zepeda, F.; Ye, R.; Samuel, E. L. G.; Yacaman, M. J.; Yakobson, B. I.; Tour, J. M. Laser-Induced Porous Graphene Films from Commercial Polymers. *Nat. Commun.* **2014**, *5* (1), 5714.
(17) Peng, L.; Xu, Z.; Liu, Z.; Guo, Y.; Li, P.; Gao, C. Ultrahigh Thermal Conductive yet Superflexible Graphene Films. *Adv. Mater.* **2017**, *29*, 1700589.
(18) Liu, Y.; Li, P.; Wang, F.; Fang, W.; Xu, Z.; Gao, W.; Gao, C. Rapid Roll-to-Roll Production of Graphene Films Using Intensive Joule Heating. *Carbon* **2019**, *155*, 462−468.
(19) Lai, L.; Li, J.; Deng, Y.; Yu, Z.; Wei, L.; Chen, Y. Carbon and Carbon/Metal Hybrid Structures Enabled by Ultrafast Heating Methods. *Small Structures* **2022**, *3* (11), 2200112.
(20) Voiry, D.; Yang, J.; Kupferberg, J.; Fullon, R.; Lee, C.; Jeong, H. Y.; Shin, H. S.; Chhowalla, M. High-Quality Graphene via Microwave Reduction of Solution-Exfoliated Graphene Oxide. *Science* **2016**, *353* (6306), 1413−1416.
(21) Liu, X.; Luo, H. Preparation of Coal-Based Graphene by Flash Joule Heating. *ACS Omega* **2024**, *9* (2), 2657−2663.
(22) Wang, N.; Samani, M. K.; Li, H.; Dong, L.; Zhang, Z.; Su, P.; Chen, S.; Chen, J.; Huang, S.; Yuan, G.; Xu, X.; Li, B.; Leifer, K.; Ye, L.; Liu, J. Tailoring the Thermal and Mechanical Properties of Graphene Film by Structural Engineering. *Small* **2018**, *14* (29), 1801346.
(23) Xiong, K.; Ma, C.; Wang, J.; Ge, X.; Qiao, W.; Ling, L. Highly Thermal Conductive Graphene/Carbon Nanotubes Films with Controllable Thickness as Thermal Management Materials. *Ceram. Int.* **2023**, *49* (6), 8847−8855.
(24) Dong, L.; Chen, Z.; Lin, S.; Wang, K.; Ma, C.; Lu, H. Reactivity-Controlled Preparation of Ultralarge Graphene Oxide by Chemical Expansion of Graphite. *Chem. Mater.* **2017**, *29* (2), 564−572.
(25) Li, J.; Liu, J.; Zhang, H.; Li, N.; Meng, Y.; Chen, Y. Highly Thermally Conductive and Flexible Reduced Graphene Oxide Films Produced Using Two-Step Liquid-Phase Repairing Method with Hydriodic Acid. *J. Mater. Sci.* **2023**, *58* (5), 2209−2221.
(26) Luo, S.; Peng, L.; Xie, Y.; Cao, X.; Wang, X.; Liu, X.; Chen, T.; Han, Z.; Fan, P.; Sun, H.; Shen, Y.; Guo, F.; Xia, Y.; Li, K.; Ming, X.; Gao, C.; Lett, N.-M. Flexible Large-Area Graphene Films of 50−600 Nm Thickness with High Carrier Mobility. *Nano-Micro Letters* **2023**, *15* (1), 61.
(27) Yang, F.; Xie, P.; Liu, X.; Zhao, H.; Liu, T.; Yin, Y.; Li, Y.; Wu, Z. High-Orientation, Defect-Rich and Porous Graphene Films for Excellent Electromagnetic Shielding and Thermal Management. *Carbon* **2023**, *214*, 118380.
(28) Zhao, P.; Peng, C.; Zhang, Q.; Fan, X.; Chen, H.; Zhu, Y.; Min, Y. Carbon-Coordinated Atomic Cobalt Directly Embedded on Carbon Cloth for Alkaline Hydrogen Evolution at High Current Density. *Chemical Engineering Journal* **2023**, *461*, 142037.
(29) Xia, T.; Cao, J.; Bissett, M.; Waring, H.; Xiang, Y.; Pinter, G.; Kretinin, A.; Yang, P.; Zhu, Y.; Zhao, X.; Hodge, S.; Thomson, T.; Kinloch, I. Graphenization of Graphene Oxide Films for Strongly Anisotropic Thermal Conduction and High Electromagnetic Interference Shielding. *Carbon* **2023**, *215*, 118496.
(30) Xiong, K.; Yang, T.; Sun, Z.; Ma, C.; Wang, J.; Ge, X.; Qiao, W.; Ling, L. Modified Graphene Film Powder Scraps for Re-Preparation of Highly Thermally Conductive Flexible Graphite Heat Spreaders. *Carbon* **2024**, *219*, 118827.
(31) Cancado, L.G.; Takai, K.; Enoki, T.; Endo, M.; Kim, Y.A.; Mizusaki, H.; Speziali, N.L.; Jorio, A.; Pimenta, M.A. Measuring the Degree of Stacking Order in Graphite by Raman Spectroscopy. *Carbon* **2008**, *46* (2), 272−275.
(32) Cançado, L. G.; Jorio, A.; Ferreira, E. H. M.; Stavale, F.; Achete, C. A.; Capaz, R. B.; Moutinho, M. V. O.; Lombardo, A.; Kulmala, T. S.; Ferrari, A. C. Quantifying Defects in Graphene via Raman Spectroscopy at Different Excitation Energies. *Nano Lett.* **2011**, *11* (8), 3190−3196.

https://doi.org/10.1021/acsami.4c10163
ACS Appl. Mater. Interfaces XXXX, XXX, XXX−XXX